

International Journal of Modern Physics D
© World Scientific Publishing Company

Challenging a Newtonian prediction through Gaia wide binaries

X. Hernandez

*Instituto de Astronomía, Universidad Nacional Autónoma de México,
Apartado Postal 70-264 C.P. 04510
México D.F. México.
xavier@astro.unam.mx*

R. A. M. Cortés

*Instituto de Astronomía, Universidad Nacional Autónoma de México,
Apartado Postal 70-264 C.P. 04510
México D.F. México.
rcortes@astro.unam.mx*

Christine Allen

*Instituto de Astronomía, Universidad Nacional Autónoma de México,
Apartado Postal 70-264 C.P. 04510
México D.F. México.
chris@astro.unam.mx*

R. Scarpa

*Instituto de Astrofísica de Canarias, c/via Lactea s/n
San Cristobal de la Laguna 38205, Spain
Departamento de Astrofísica, Universidad de La Laguna (ULL)
38206 La Laguna, Tenerife, Spain.
riccardo.scarpa@gtc.iac.es*

Received Day Month Year

Revised Day Month Year

Under Newtonian dynamics, the relative motion of the components of a binary star should follow a Keplerian scaling with separation. Once orientation effects and a distribution of ellipticities are accounted for, dynamical evolution can be modelled to include the effects of Galactic tides and stellar mass perturbers, over the lifetime of the solar neighbourhood. This furnishes a prediction for the relative velocity between the components of a binary and their projected separation. Taking a carefully selected small sample of 81 solar neighbourhood wide binaries from the *Hipparcos* catalogue, we identify these same stars in the recent Gaia DR2, to test the prediction mentioned using the latest and most accurate astrometry available. The results are consistent with the Newtonian prediction for projected separations below 7000 AU, but inconsistent with it at larger separations, where accelerations are expected to be lower than the critical $a_0 = 1.2 \times 10^{-10} \text{ m s}^{-2}$ value of MONDian gravity. This result challenges Newtonian gravity at low accelerations and shows clearly the appearance of gravitational anomalies of the type usually attributed to dark matter at galactic scales, now at much smaller

2 *X. Hernandez et al.*

stellar scales.

Keywords: Gravitation; star binary; general.

PACS numbers: 04.50.Kd, 95.35.+d, 97.10.Vm, 97.80.d

1. Introduction

In galactic dynamics, the range of systems over which gravitational anomalies appear in the low acceleration regime extends across vast astronomical scales. Ultra faint dwarf galaxies with scale radii of order a few tens of parsecs show stellar velocity dispersions implying Newtonian mass to light ratios in the hundreds or even thousands (e.g. Ref. 1). The classical dwarfs have sizes of order of a kpc and mass to light ratios derived from observed stellar kinematics inconsistent with those of naked stellar populations under standard gravity by well over an order of magnitude (e.g. Ref. 2). This reflects what is observed in spiral galaxies at tens of kpc, where rotation curves (e.g. Ref. 3) again yield dynamics not corresponding to Newtonian dynamics given the empirically determined matter content. The trend has been recently extended to include elliptical galaxies observed out to their external low acceleration regions by Ref. 4, and even for the case of Galactic globular clusters where velocity dispersion profiles suggest a change away from Newtonian dynamics for low accelerations (e.g. Ref. 5, Ref. 6).

Empirically, the above gravitational anomalies can be described by MONDian dynamics (Ref. 7, Ref. 8), where below an acceleration threshold of $a_0 = 1.2 \times 10^{-10} \text{ m s}^{-2}$ kinematics stop falling along Newtonian expectations of $v \propto R^{-1/2}$ to flatten out at the Tully-Fisher values of $V_{TF} = (GMa_0)^{1/4}$ for centrifugal equilibrium velocities or corresponding velocity dispersions for pressure supported systems, where M is the total baryonic mass of the system in question. The standard interpretation of **these observations is the presence** of dominant halos of a yet undetected hypothetical dark matter component surrounding the astrophysical systems being observed.

Wide binary pairs in the solar neighbourhood offer an opportunity to probe dynamics at low accelerations on the smallest astrophysical scales. In principle these can yield crucial restrictions on the structure of gravity at low accelerations and lengths where the presence of dark matter is not expected. For a solar mass binary, at separations of above $3.4 \times 10^{-2} \text{ pc}$, 7000 AU, accelerations will fall below a_0 under Newtonian expectations. A first attempt in this direction was made by two of us in Ref. 9 where we used the Ref. 10 -henceforth SO11- carefully selected sample of *Hipparcos* wide binaries. This catalogue includes a full Bayesian model and use of local 5-dimensional phase space density to identify wide binary candidates and rigorously assign a probability that each candidate forms a physical system, rather than being the result of chance associations.

Retaining a sample of binaries from SO11 where contamination was limited to less than 10%, in Ref. 9 results indicated relative velocities for the binary pairs stud-

ied above the Newtonian expectations for accelerations below a_0 . This remained true even after accounting for projection effects, ellipticity distributions and disruption and evolution of ionised binaries due to the Galactic tidal field and encounters with field stars and stellar remnants, as modelled by Ref. 11, albeit the relatively large errors in proper motions present in the *Hipparcos* catalogue.

One of us, in Ref. 12, explored the problem using a small sample of 60 candidate wide binaries with projected separations between 0.004 and 1.0 pc. That study found that a number of wide binaries are capable of surviving the galactic tides and stellar encounters of the solar neighbourhood dynamical environment, with a small sub-sample of the widest pairs showing kinematics more consistent with MONDian dynamics than Newtonian ones. More recently, theoretical studies by Ref. 13 and Ref. 14 confirmed that Gaia data, in terms of expected number of detected wide binaries and confidence intervals for the relevant proper motions and parallaxes, are sufficient to detect MONDian deviations from Newtonian dynamics in the low acceleration regime probed by these systems, should they be present.

The obvious next step is to reproduce the careful and detailed procedure presented in SO11, but using this time the Gaia DR2 catalogue. This painstaking approach will ultimately furnish a definitive answer regarding the presence of gravitational anomalies at stellar scales in the low acceleration regime, but is currently hampered by our incomplete understanding of the problems still present in the data of the very novel Gaia DR2. For example, only about two thirds of the *Hipparcos*2 sources have Gaia DR2 counterparts (Ref. 15). Also, Gaia treats all binaries closer than about 1" (depending on the magnitude difference) as single sources, which may give anomalous parallaxes, and the parallax solutions may be more sensitive to duplicity in certain areas, etc. (see Ref. 16 A1 for some of the known issues.)

A first order sampling of the issue can be more directly probed by taking advantage of the correspondence between the Gaia and the *Hipparcos* catalogues. One can take the sample selection from the accurate Bayesian analysis of SO11, and the actual astrometric data from the Gaia DR2. Here we present results of such an approach, yielding a small sample of 81 wide binaries from the original SO11 catalogue having a $< 10\%$ probability of being chance associations, Gaia DR2 data consistent with the original *Hipparcos* reported quantities, and consistent parallaxes for both components in the Gaia DR2. Although it is only a reduced sample, the superior quality of the Gaia satellite allows us to infer relative velocities for the binaries in question to a much higher degree of accuracy than what was available to Ref. 9. Interestingly, our results show a departure from Newtonian predictions as projected separations grow beyond the critical 0.034 pc. Indeed, our new results are consistent with what was reported in Ref. 9: the mean values of the inferred relative velocities are essentially unchanged, with the error bars showing a dramatic reduction. This effectively rules out the Newtonian prediction of Ref. 11 and provides solid evidence for a gravitational anomaly in the low acceleration regime, this time at stellar scales.

2. Sample selection

As outlined in the introduction, the sample selection is based on the wide binary catalogue of SO11, which was constructed using a very detailed Bayesian procedure. This identifies and quantifies the probability of each binary pair being an actual physical system, rather than the result of projection effects or chance associations, including also the Tycho-2 and the *Tycho* double star catalogues (Ref. 17 and Ref. 18). To that end a 5-dimensional space of spatial positions and proper motions was cross-correlated with a galactic phase-space density library, explicitly excluding the largest known local star clusters, to identify binary candidates as significant local over-densities in phase space. Corrections due to spherical projections effects were also considered, to yield a catalogue of 840 wide binaries with projected separations of between 0.003 and 10 pc and, crucially, a well determined probability of chance association, P_{ch} . Taking only those pairs where this probability satisfies $P_{ch} < 10\%$, reduces the original SO11 sample to 359 wide binaries. This catalogue is also narrowly restricted in spectral type for both primaries and companions of each binary, yielding stars in a narrow range of masses centred on $0.5M_{\odot}$. This last is important as it allows a clean comparison to the fixed mass binary simulations of Ref. 11, see below. Following the original SO11 terminology, the brightest star in each binary system is termed the primary.

The SO11 search criteria ensure the absence of near neighbours, and result in binary candidates with separations which are always many times smaller than the typical interstellar separations at the location of the binaries in question. Extensive testing with synthetic samples in SO11 guarantees the catalogue includes very few multiple systems with undetected extra companions and is highly complete in the 6 to 100 pc distance range from the Sun.

We now take advantage of the *Hipparcos* to Gaia DR2 correspondence availability to search for the updated astrometry of the 359 $P_{ch} < 10\%$ wide binary SO11 sample in the Gaia DR2. The search returns only 151 pairs where each component of the SO11 binaries appears in the Gaia DR2 with two proper motion parameters and measured parallax. This is not surprising, since only about two thirds of the *Hipparcos*2 sources have Gaia DR2 counterparts (Ref. 15). It is not yet clear why there are so many sources missing. According to the above authors a combination of effects may be present. As each binary is excluded if either component is absent from the DR2, the fraction we obtain is typical. Next, the SO11 catalogue returns a few systems where more than one secondary is identified as the companion to a given primary, and also cases where a single secondary is identified as the companion to more than one primary. We remove all these cases of multiple identifications, bringing the sample down to 131 binaries.

A first test of the reliability with which the *Hipparcos* binaries have been identified in the Gaia DR2 comes from comparing the proper motion measurements reported in SO11 with the corresponding measurements reported in the Gaia DR2. This is shown in Figures 1 and 2, where the ranges shown in the axes were chosen

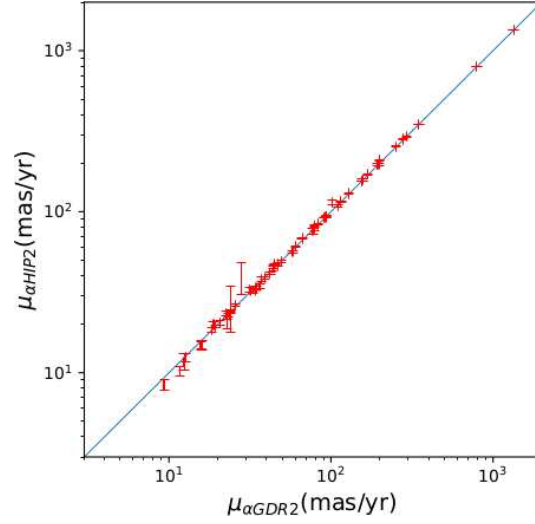


Fig. 1. Comparison of SO11 *Hipparcos* and Gaia DR2 proper motion data in right ascension for each of the two components of the binaries studied. The agreement with the identity line in the majority of cases shows the stars in question have been successfully identified from the first catalogue to the Gaia DR2 sample.

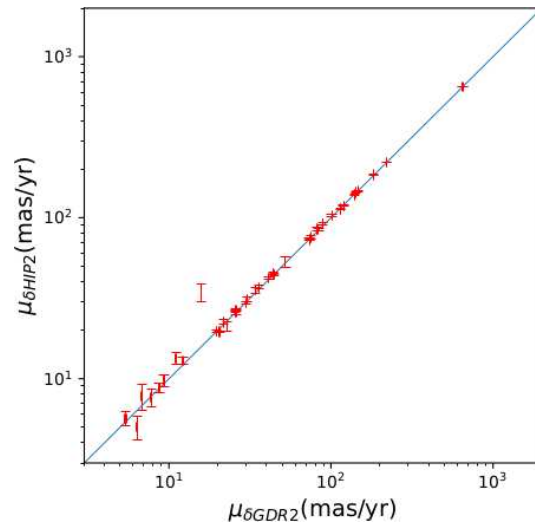


Fig. 2. Comparison of SO11 *Hipparcos* and Gaia DR2 proper motion data in declination for each of the two components of the binaries studied. The agreement with the identity line in the majority of cases shows the stars in question have been successfully identified from the first catalogue to the Gaia DR2 sample.

so as to display clearly most of our sample; a handful of very discordant systems do not appear in the plots, as they are very far from the identity line shown. It is clear that in most cases, the proper motion values reported by both satellites are in agreement with each other, to within their respective confidence intervals, the *Hipparcos* error ranges being much larger than the Gaia DR2 ones. Still, we introduce a cut to remove from consideration any binary candidate where for any component the *Hipparcos* and Gaia DR2 **proper motions** are more than 3σ from each other. Our final results are not sensitive to this threshold, provided the few discordant misidentified binaries are removed. This cut leaves us with only 117 stellar pairs. Next, as shown in Figure 3, we check that the Gaia DR2 reported parallax measurements for each of the primaries and companions are not discordant, and remove from the sample any binary where the distances to each component are not within 13% of each other. This exclusion criterion identifies 17 candidates, thus reducing the sample to 100 pairs. Notice that the test shown in Figures 1 and 2 effectively gives us a 10 year baseline which, on top of the robustness in the SO11 catalogue towards multiple systems, where no radial velocities are involved, removes any remaining binary where a third component might be altering proper motions with timescales shorter than 10 years (see Ref. 14).

Finally, we take advantage of the Gaia radial velocity measurements (when available) and remove any binaries where the radial velocity difference, ΔV_r , between both components is larger than 4 km s^{-1} . The resulting cut is not very sensitive to this velocity threshold, as the removed binary pairs typically have much larger and

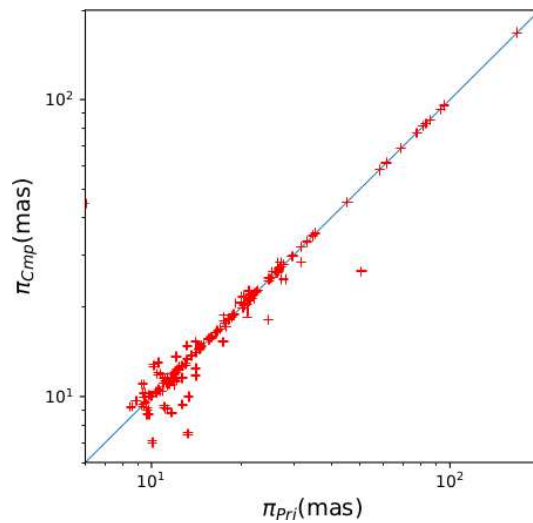


Fig. 3. Comparison of the Gaia DR2 reported parallax for the two distinct components of each of the binaries studied. The disagreement of only a handful of cases with the identity line allows to exclude such discordant pairs as part of the expected 10% misidentified binaries in the original SO11 catalogue, or as misidentified stars in going from the *Hipparcos* catalogue to the Gaia DR2.

discordant ΔV_r values, with an average value for those removed of $\Delta V_r = 28 \text{ km s}^{-1}$. Our final sample comprises 81 binary pairs.

Thus, we have preferred very strict cuts to our final sample which leave us with modest numbers, but guarantee the exclusion of misidentified stars in going from *Hipparcos* data to Gaia DR2 and chance alignment contamination in the original SO11 catalogue, all of which become conspicuous in the comparisons presented in this section. Table 1 summarises the Gaia DR2 properties used and catalogue numbers from both *Hipparcos* and Gaia for the primaries and companions of all the binaries used, together with the results of the exclusion criteria described.

3. Gaia wide binary projected kinematic results

In Ref. 9 we calculated the projected separation in the plane of the sky using only the parallax to the primary of each binary, but given the higher quality Gaia DR2 data, we now compute the projected separation between the components of each binary using explicitly the observed Gaia positions and parallaxes to each component of the binary. The average parallax to both components is used to gauge the distance to each pair. Using reported Gaia proper motions, the relative velocity difference in one dimension is calculated for each binary twice, once considering only right ascension proper motions, and once considering only declination proper motions. In all cases the relative physical motion is calculated including full spherical geometric effects (e.g. Ref. 19), and not under the more standard small angle approximation. This requires the radial velocity of at least one component, which we have for 71 of our 81 final pairs. For the remaining 10, a $V_r = 0$ was assumed for the effects of the above correction (e.g. SO11). The effects of the above refinement are only relevant for the nearest and widest of pairs, in our sample only a few individual systems, as

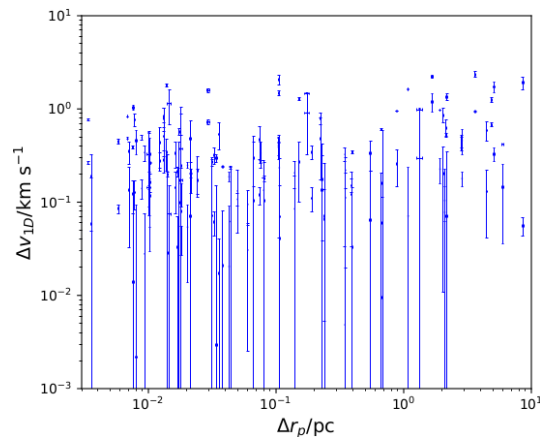


Fig. 4. One dimensional relative velocities for the final binary sample, showing both results from using only right ascension data, and from using only declination values, with corresponding error bars.

can be **readily checked** from the data used and shown in Table 1.

Figure 4 gives the two Δv_{1D} measurements for each binary pair in the final sample, with corresponding 1σ error bars. A clear flat upper envelope is evident. In Figure 5 we show the rms. value for the one dimensional velocity differences described above, plotted against projected separations in a binned logarithmic scale, circles and triangles for right ascension and declination data, respectively. The horizontal error bars give the bin sizes, while the vertical ones show the contribution of Gaia reported errors and error propagation, to which a Poisson contribution has been added, and which given the small numbers of binaries in each bin (21, 23, 17, 8 and 12, from left to right), actually dominates the error budget in most cases. The dashed vertical line appears at 7000 AU, the approximate scale where acceleration is expected to drop below a_0 .

Also shown in Figure 5 are the Newtonian predictions for this same quantity from Ref. 11, where large collections of 50,000 simulated binaries are modelled for a range of plausible distributions of ellipticities, and followed dynamically under Newtonian expectations within the local Galactic tidal field. These are also subject to the effects of field star and field stellar remnant bombardment for a 10 Gyr period. Finally, the resulting bound and un-bound stellar pairs are projected along a fiducial line of sight to yield a robust prediction for the expected $\langle \Delta v_{1D}^2 \rangle^{1/2}$ as a function of Δr , solid curve. This results are easy to understand; a $\Delta v \propto \Delta r^{-1/2}$ trend is apparent, down to the tidal radius of the problem which appears at 1.7

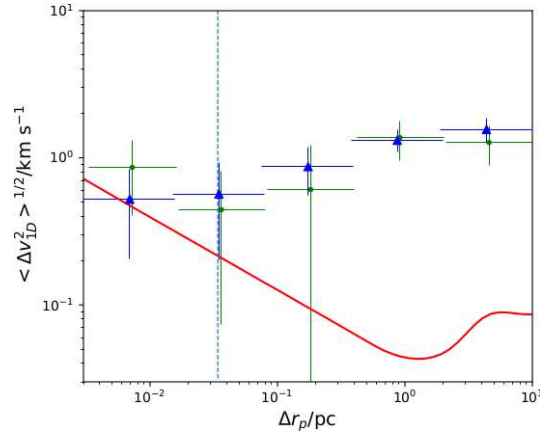


Fig. 5. The solid curve shows the rms. value for the one dimensional relative velocity between the components of a present day Solar Neighbourhood binary as a function of projected separation, for the Newtonian prediction of Ref. 11. The same quantity for the SO11 wide binary catalogue stars, this time using Gaia DR2 data, is shown by the points with error bars, circles for right ascension data and triangles for declination. A small artificial horizontal offset was introduced on both data sets to avoid having overlapping error bars. The inconsistency of the observed data with the Newtonian prediction is obvious, for separations greater than the 7000 AU at which accelerations are expected to drop below a_0 . This threshold is indicated by the dashed vertical line.

pc. Beyond this point, ionised binaries continue to move along practically common Galactic orbits, with relative velocities which show a mild enhancement which then levels off at close to 0.1 km s^{-1} .

It is clear that to the left of the a_0 dashed line, our results are consistent within confidence intervals with the Newtonian expectations. However, going to separations larger than 7000AU, the observed points stop following the expected trend and actually level off at a Δv amplitude close to the values seen at the a_0 point, reproducing qualitatively the phenomenology seen in galactic rotation curves.

This result for the binary sample presented is extremely challenging to a Newtonian point of view, where the relative velocities are expected to be much lower than observed. Given the construction of the SO11 sample, binaries with small velocity differences would appear as stronger local over-densities in phase space, and hence, selection criteria, if anything, are biased against binaries with large velocity differences, not small ones. Thus, from a Newtonian point of view, bound binaries with separations smaller than the tidal radius of 1.7 pc and larger than 7000 AU are unexpectedly missing. Also, as already mentioned in Ref. 20, a population of non-chance associated binaries appears at scales above 7000AU having relative velocities over an order of magnitude above bound expectations, with relative velocities of $\sim 1 \text{ km s}^{-1}$ and separations of a few pc; the dynamical ages of un-bound systems are of only a few 10^6 years. What sustains and replenishes these populations under a Newtonian framework? At separations below the 1.7 pc tidal radius of the problem, bound binaries should appear, under a Newtonian framework.

Furthermore, the results shown in figure 5 confirm what was presented in Ref. 9, though the much coarser *Hipparcos* data of that first study yielded significantly larger error bars. That those first results might have been the result of missed biases or simply the error structure of the *Hipparcos* data now appears very unlikely, as we see two consistent results coming from data obtained by two completely independent satellites. Indeed, the error bars have significantly shrunk, with central results changing little. Note also that the two Δv_{1D} estimates we obtain, using only right ascension or only declination data, are consistent with each other.

A potential caveat on the interpretation presented comes from the possible presence of a population of misidentified binaries being actually parts of loose, dissolving moving groups. Ref. 20 recently showed that although isolated wide binaries dominate, a search algorithm of the type used in SO11 could also pick up a fraction of misidentified binaries being part of larger moving groups, many of the smallest of which probably remain undiscovered. A full answer and validation or otherwise of our results, necessarily awaits a much more extensive study through the full Gaia catalogue, and a more complete exploration and understanding of the phase-space structure and over-densities of the Solar Neighbourhood and local Milky Way disk environment.

Although the gravitational anomaly detected appears on crossing the a_0 threshold of MOND, in MOND as such, the results are equally unexpected as the external field effect of MOND (or AQUAL e.g. Ref. 8 should dominate. Given that the or-

bital acceleration of the solar neighbourhood is higher than the internal acceleration of the binaries in question, in MOND as such, only a very modest enhancement of the effective value of G would be expected (e.g. Ref. 13). Thus, within a MONDian frame our results imply the validity of not the most well studied version, but rather of a variant where the external field effect does not appear, or is much suppressed e.g. as in Ref. 21. In terms of covariant extensions to GR having a MONDian low velocity limit, it is hard to know to what extent an external field effect might be present in many of the recently developed options (e.g. the $f(R)$ variants reviewed in Ref. 22, the emergent gravity of Ref. 23 or the $F(R,L)$ proposal of Ref. 24. Our results then serve as constraints in terms of requiring a minimal external field effect, at least for the sub-parsec scales in the solar neighbourhood explored.

4. Final remarks

We have presented a sample of 81 wide binaries which were very carefully selected against chance associations or projection effects through the cross correlation of the *Hipparcos*, *Tycho-2* and the *Tycho* double star catalogues, amongst others, with the detailed 5-dimensional phase space structure of the solar neighbourhood by SO11. By taking advantage of the cross-identification of the *Hipparcos* catalogue and the Gaia DR2 data, we updated the parallax and proper motion observations of SO11 to use exclusively Gaia DR2 astrometry.

These binaries were then compared to Newtonian predictions for the expected one dimensional rms. relative velocity between the components of each binary and their projected separations, including modeling orientation effects, a number of plausible distributions of ellipticities and, crucially, the effects of Galactic tides and stellar and stellar remnant perturbers over a 10 Gyr period, by Jiang & Tremaine (2010).

For separations below 7000 AU, where accelerations are expected to be above the $a_0 = 1.2 \times 10^{-10} \text{ m s}^{-2}$ of MOND, we find the data to be consistent with the Newtonian predictions. For projected separations above 7000 AU, however, the data are inconsistent with Newtonian predictions. This challenges the validity of Newtonian dynamics at the low acceleration regime, and shows the existence of gravitational anomalies of the type generally attributed to the presence of a hypothetical and dominant dark matter component, this time down to the relatively tiny sub-parsec stellar scales.

Index	HIP2	GDR2	α	δ	μ_α	μ_δ	v_r	d	$\log_{10}(\Delta R)$	Exclusion
SO11			(deg)		(mas/yr)		(km/s)	(pc)		Test
16	15371	4722135642226356736	49.565826	-62.503574	1331.151 \pm 0.355	648.523 \pm 0.431	12.01 \pm 0.32	12.046 \pm 0.027		
	15330	4722111590409480064	49.454851	-62.572523	1337.591 \pm 0.142	649.930 \pm 0.154	12.21 \pm 0.17	12.039 \pm 0.011	-1.744 \pm 0.002	
17	17414	43335880716390784	55.969727	16.670667	157.945 \pm 0.086	-316.326 \pm 0.052	34.18 \pm 0.15	17.209 \pm 0.012		
	17405	43335537119008896	55.939232	16.665933	156.215 \pm 0.089	-310.291 \pm 0.064	34.22 \pm 1.08	17.239 \pm 0.014	-2.051 \pm 0.001	
21	19859	3285218186904332288	63.869527	6.186399	-109.700 \pm 0.095	-107.368 \pm 0.079	-7.21 \pm 0.15	22.087 \pm 0.026		
	19855	3285218255623808640	63.857006	6.199170	-101.763 \pm 0.080	-111.982 \pm 0.055	-7.93 \pm 0.16	22.104 \pm 0.022	-2.163 \pm 0.001	
22	23693	4763906879239461632	76.377477	-57.472197	-32.140 \pm 0.276	117.417 \pm 0.310	-1.15 \pm 0.22	11.625 \pm 0.020		
	23708	4763897739549071744	76.447122	-57.553318	-32.784 \pm 0.049	119.633 \pm 0.054	-0.88 \pm 0.16	11.698 \pm 0.003	-1.740 \pm 0.001	
25	25278	3400292798990117888	81.107227	17.383504	250.765 \pm 0.316	-7.332 \pm 0.209	37.67 \pm 0.24	14.585 \pm 0.037		
	25220	3394298532176344960	80.911047	17.324092	251.000 \pm 0.092	-5.778 \pm 0.068	37.94 \pm 0.13	14.565 \pm 0.011	-1.301 \pm 0.001	
28	26690	3395863205942142976	85.075658	15.350146	2.551 \pm 0.100	-36.058 \pm 0.080		167.953 \pm 2.110		
	26844	3347826784173590656	85.495633	15.337041	79.115 \pm 0.087	-43.071 \pm 0.068		22.423 \pm 0.025	-0.172 \pm 0.010	c
29	26779	263916708025623680	85.334752	53.478804	2.784 \pm 0.075	-523.602 \pm 0.072	1.07 \pm 0.18	12.280 \pm 0.007		
	26801	263916742385357056	85.378072	53.487581	3.915 \pm 0.078	-515.938 \pm 0.078	1.92 \pm 0.27	12.278 \pm 0.008	-2.234 \pm 0.001	
65	62229	6060965699625586176	191.308450	-57.355867	-201.033 \pm 0.052	-131.548 \pm 0.046	14.76 \pm 0.16	19.808 \pm 0.018		
	69570	6092573252981419776	213.602784	-48.147162	-102.218 \pm 0.095	-121.897 \pm 0.120	-23.92 \pm 0.13	37.842 \pm 0.087	0.910 \pm 0.002	c,d
73	70529	1254695603704323712	216.434870	23.612274	792.548 \pm 0.092	-1116.601 \pm 0.111	8.78 \pm 0.21	16.346 \pm 0.014		
	70536	1254694882149817728	216.448113	23.615657	793.487 \pm 0.085	-1119.010 \pm 0.095		16.339 \pm 0.014	-2.445 \pm 0.004	
80	79755	1642641410934267008	244.172569	67.239204	-498.018 \pm 0.050	84.110 \pm 0.053	-19.86 \pm 0.19	10.768 \pm 0.004		
	79762	1642642957122493824	244.183431	67.256628	-483.168 \pm 0.066	89.266 \pm 0.072		10.765 \pm 0.005	-2.473 \pm 0.001	
81	80337	6018047019138644480	246.005789	-39.192966	74.146 \pm 0.306	3.666 \pm 0.226	12.89 \pm 0.13	12.908 \pm 0.023		
	80300	6018034958869558912	245.891422	-39.229487	77.135 \pm 0.147	0.334 \pm 0.110		12.914 \pm 0.012	-1.666 \pm 0.001	
85	83591	4364527594192166400	256.260183	-5.071414	-916.562 \pm 0.155	-1138.804 \pm 0.104	34.14 \pm 0.15	10.466 \pm 0.007		
	83599	4364480521350598144	256.303450	-5.099110	-917.276 \pm 0.098	-1131.947 \pm 0.065	34.44 \pm 0.44	10.456 \pm 0.006	-2.029 \pm 0.001	
87	84405	4109030160308317312	258.835189	-26.607739	-466.541 \pm 0.646	-1142.063 \pm 0.451		5.960 \pm 0.008		
	84478	4109034455276324608	259.053369	-26.550990	-479.850 \pm 0.101	-1124.545 \pm 0.068	-0.04 \pm 0.22	5.950 \pm 0.003	-1.675 \pm 0.001	b
112	493	2797111130991722240	1.477436	18.234370	-150.936 \pm 0.121	-147.985 \pm 0.089	-45.70 \pm 0.16	37.429 \pm 0.102		
	495	2773086595766697856	1.480470	18.075245	-147.614 \pm 0.094	-145.798 \pm 0.079	-45.00 \pm 0.74	37.683 \pm 0.085	-0.982 \pm 0.002	
130	7699	4911275281704066048	24.782478	-56.429512	91.146 \pm 0.041	-31.652 \pm 0.041	9.48 \pm 0.31	46.855 \pm 0.061		
	6485	4909846500703006976	20.839305	-57.480902	92.790 \pm 0.045	-36.082 \pm 0.038	8.62 \pm 0.21	45.315 \pm 0.053	0.284 \pm 0.001	
132	9487	2517584007848935808	30.511899	2.763759	32.692 \pm 0.940	-2.895 \pm 0.821		50.506 \pm 1.707		b
	9519	2517585927699042944	30.611532	2.815808	36.368 \pm 0.126	-10.811 \pm 0.098	4.58 \pm 0.16	48.404 \pm 0.137	-1.014 \pm 0.016	
140	11477	4967177781457918976	37.007194	-33.811016	18.526 \pm 0.121	5.163 \pm 0.193		47.258 \pm 0.315		
	11448	4967153630858709120	36.926542	-33.896542	18.383 \pm 0.030	4.481 \pm 0.052	12.26 \pm 0.17	47.708 \pm 0.075	-1.046 \pm 0.004	b
155	15304	10584899657116672	49.360666	7.655784	166.360 \pm 0.071	-6.237 \pm 0.062	31.35 \pm 0.20	47.288 \pm 0.092		
	15310	10608573516849536	49.387317	7.690127	168.749 \pm 0.073	-6.314 \pm 0.063	31.90 \pm 0.15	47.269 \pm 0.088	-1.447 \pm 0.002	
157	15527	5060104351007433472	50.016623	-28.854353	349.057 \pm 0.036	-65.299 \pm 0.041	39.89 \pm 0.13	36.024 \pm 0.041		
	15526	5060105892897388288	50.013976	-28.784118	348.847 \pm 0.065	-66.663 \pm 0.076	40.31 \pm 0.14	36.009 \pm 0.052	-1.355 \pm 0.001	
173	22534	4777112872882315264	72.734825	-53.459330	-80.769 \pm 0.929	85.658 \pm 0.968	6.44 \pm 3.13	38.970 \pm 0.624		
	22562	4777119126354782592	72.835038	-53.405518	-82.413 \pm 0.043	83.684 \pm 0.052	10.70 \pm 0.49	38.006 \pm 0.032	-1.268 \pm 0.008	d
175	24046	3422042582096699520	77.517088	27.556119	197.860 \pm 0.093	-89.579 \pm 0.056	15.64 \pm 0.16	40.470 \pm 0.074		
	24035	3422047495539178496	77.504564	27.642799	198.179 \pm 0.596	-88.591 \pm 0.357	21.24 \pm 0.43	40.295 \pm 0.457	-1.210 \pm 0.006	a,b,d
187	33705	5607190344506642432	105.040814	-31.141532	18.789 \pm 0.043	35.596 \pm 0.049	16.61 \pm 0.17	38.123 \pm 0.043		
	33691	5607189485513198208	105.011544	-31.227929	18.893 \pm 0.061	36.119 \pm 0.065	16.83 \pm 0.21	38.356 \pm 0.061	-1.222 \pm 0.001	
190	34714	890422213103244544	107.830615	33.111833	-110.510 \pm 0.075	-7.495 \pm 0.066	3.05 \pm 0.24	45.125 \pm 0.095		
	34700	890346243721923968	107.810770	32.614987	-110.866 \pm 0.102	-6.789 \pm 0.088	3.02 \pm 0.33	44.748 \pm 0.143	-0.409 \pm 0.002	
195	37718	5493209501673364736	116.051359	-50.456108	-114.435 \pm 0.047	143.459 \pm 0.042	8.69 \pm 0.37	30.084 \pm 0.022		
	37727	5493209437253410432	116.067894	-50.466001	-111.783 \pm 0.060	142.603 \pm 0.053	9.16 \pm 0.30	30.080 \pm 0.027	-2.120 \pm 0.002	
201	42401	5746824674801810816	129.688303	-13.256527	-63.858 \pm 0.051	38.374 \pm 0.041	20.53 \pm 0.25	31.596 \pm 0.032		
	41662	5751951182125903872	127.418304	-9.976270	-56.556 \pm 0.064	34.122 \pm 0.050	2.30 \pm 0.24	35.328 \pm 0.055	0.364 \pm 0.001	d
204	43970	610526719204475136	134.312562	15.322854	60.337 \pm 0.292	19.748 \pm 0.221		48.401 \pm 0.415		

Continued on next page

Index	HIP2	GDR2	α	δ	μ_α	μ_δ	v_r	d	$\log_{10}(\Delta R)$	Exclusion
SO11			(deg)		(mas/yr)		(km/s)	(pc)		Test
	44001	610549499710989440	134.396934	15.581374	60.440 \pm 0.161	20.509 \pm 0.106		48.801 \pm 0.233	-0.638 \pm 0.006	
207	44858	692119656035933568	137.099198	27.535750	-53.239 \pm 0.128	71.659 \pm 0.096	30.02 \pm 0.22	48.891 \pm 0.237		
	44864	692120029700390912	137.112900	27.543447	-51.819 \pm 0.113	73.524 \pm 0.074	30.31 \pm 0.14	49.124 \pm 0.230	-1.910 \pm 0.007	
215	51312	749786562715192320	157.213545	34.885408	-111.186 \pm 0.069	-62.017 \pm 0.069	4.11 \pm 0.17	49.344 \pm 0.126		
	52140	748360706587700352	159.782027	32.832960	-110.338 \pm 0.106	-58.939 \pm 0.087	-0.60 \pm 0.17	50.382 \pm 0.138	0.411 \pm 0.002	d
218	52787	3550081879381593728	161.879229	-22.348154	-124.690 \pm 0.115	-28.341 \pm 0.084	23.85 \pm 0.25	33.612 \pm 0.085		
	52776	3550084490721711872	161.855204	-22.286843	-124.539 \pm 0.112	-29.837 \pm 0.070	23.24 \pm 0.52	33.603 \pm 0.079	-1.417 \pm 0.002	
224	55765	3967618155853506304	171.400912	16.456513	-142.347 \pm 0.204	-5.645 \pm 0.179	18.88 \pm 0.67	47.198 \pm 0.296		
	55262	3965063921622777856	169.776912	13.390754	-146.589 \pm 0.080	-0.006 \pm 0.069	8.33 \pm 0.21	47.472 \pm 0.093	0.454 \pm 0.004	d
229	58067	3975129194660883328	178.631559	19.411157	-450.502 \pm 0.095	-16.554 \pm 0.069	5.94 \pm 0.29	39.622 \pm 0.082		
	58073	3975223065466473216	178.644111	19.427759	-450.600 \pm 0.083	-15.497 \pm 0.058	5.76 \pm 0.22	39.601 \pm 0.071	-1.851 \pm 0.002	
230	58085	5236197322996128128	178.686141	-66.376482	13.792 \pm 0.037	-65.816 \pm 0.036	-6.80 \pm 0.37	44.078 \pm 0.047		b
	58121	5236196498362394112	178.814952	-66.409354	12.724 \pm 0.048	-63.279 \pm 0.045	-7.63 \pm 0.13	44.016 \pm 0.063	-1.328 \pm 0.001	
245	64057	3945118265299248128	196.914217	24.010449	-261.638 \pm 0.077	148.003 \pm 0.059	-1.68 \pm 0.15	37.442 \pm 0.053		
	64059	3945118643256370688	196.918496	24.020558	-262.455 \pm 0.078	146.042 \pm 0.054	-1.70 \pm 0.13	37.433 \pm 0.051	-2.150 \pm 0.003	
253	67246	3721126409323324416	206.735799	6.349899	-510.447 \pm 0.071	-110.225 \pm 0.064	-30.42 \pm 0.20	31.489 \pm 0.039		
	67291	3721114933170707328	206.867792	6.315179	-509.440 \pm 0.083	-111.022 \pm 0.061	-30.67 \pm 0.15	31.332 \pm 0.045	-1.128 \pm 0.001	
264	73365	1586977844504888576	224.886978	45.464606	-33.680 \pm 0.043	100.046 \pm 0.044	-18.94 \pm 0.14	33.745 \pm 0.027		
	73360	1586977737129182848	224.877247	45.448463	-35.321 \pm 0.037	101.074 \pm 0.039	-18.99 \pm 0.26	33.768 \pm 0.024	-1.986 \pm 0.002	
270	74666	1278391075716738560	228.876113	33.314351	82.549 \pm 0.554	-111.909 \pm 0.560		37.342 \pm 0.531		a
	74674	1278392381386793856	228.910214	33.320448	82.776 \pm 0.040	-110.040 \pm 0.044	-11.83 \pm 0.18	36.948 \pm 0.042	-1.724 \pm 0.009	
271	75104	1277115023753077248	230.207752	31.480707	-179.339 \pm 0.036	139.058 \pm 0.039	-26.82 \pm 0.17	45.885 \pm 0.055		
	75011	1277185633015465856	229.916339	31.843109	-181.021 \pm 0.033	139.573 \pm 0.042	-26.32 \pm 0.19	45.433 \pm 0.057	-0.456 \pm 0.001	
284	79958	5931674608438449792	244.816099	-55.504655	5.669 \pm 0.067	18.412 \pm 0.051	-0.31 \pm 0.52	28.113 \pm 0.029		
	80365	5831891213733627264	246.077754	-59.344070	-3.205 \pm 0.063	-5.572 \pm 0.052		7649.524 \pm 2501.324	2.417 \pm 0.283	c
298	85620	1440518669436791296	262.435226	63.851870	1.533 \pm 0.049	-182.061 \pm 0.053	-34.02 \pm 0.16	45.738 \pm 0.051		
	85575	1440425863783337856	262.319088	63.868353	0.864 \pm 0.053	-181.967 \pm 0.060	-33.72 \pm 0.18	45.663 \pm 0.060	-1.368 \pm 0.001	
309	92388	4505477838068264064	282.408880	13.217640	-199.313 \pm 0.096	-223.979 \pm 0.102	-54.54 \pm 0.21	37.760 \pm 0.068		
	92638	4312046495498949888	283.121483	11.209184	-189.830 \pm 0.070	-224.477 \pm 0.079	-22.45 \pm 0.90	38.302 \pm 0.065	0.150 \pm 0.002	d
314	94150	6421542154150684160	287.472100	-68.424635	155.088 \pm 0.122	-42.976 \pm 0.141	-9.61 \pm 0.12	36.982 \pm 0.122		
	94154	6421555485729063424	287.479128	-68.299872	155.710 \pm 0.036	-41.937 \pm 0.046	-9.28 \pm 0.13	36.655 \pm 0.041	-1.096 \pm 0.002	
322	97384	4240508901699614976	296.888713	1.087910	-28.713 \pm 0.067	-226.754 \pm 0.046		47.116 \pm 0.093		
	95829	4287506873404614784	292.359656	0.527119	-25.932 \pm 0.072	-237.555 \pm 0.070		44.067 \pm 0.083	0.560 \pm 0.002	
323	97940	4240626686883261184	298.562299	1.942265	-1.562 \pm 0.085	-270.206 \pm 0.052	9.55 \pm 0.16	40.151 \pm 0.097		
	97950	4240625896609242624	298.607267	1.940219	-0.186 \pm 0.077	-269.831 \pm 0.047	10.20 \pm 0.20	40.047 \pm 0.087	-1.502 \pm 0.002	
325	99171	4236276194243977344	302.008090	-0.678476	115.520 \pm 0.095	-67.593 \pm 0.060	-3.27 \pm 0.14	46.678 \pm 0.137		
	99100	4235895935019949952	301.788725	-0.874544	115.276 \pm 0.104	-67.915 \pm 0.050	-3.08 \pm 0.14	46.633 \pm 0.144	-0.621 \pm 0.003	
326	99572	6879764552737781888	303.108646	-12.618340	193.068 \pm 0.111	-195.497 \pm 0.064	27.30 \pm 0.16	28.249 \pm 0.054		
	99550	6879662263797806976	303.040242	-12.893999	192.627 \pm 0.068	-193.957 \pm 0.045	27.53 \pm 0.25	28.248 \pm 0.033	-0.854 \pm 0.001	
331	100896	4228891667990334976	306.864400	-2.103364	-64.779 \pm 0.352	-67.523 \pm 0.216		49.464 \pm 0.479		
	100895	4228891221313732864	306.861958	-2.119817	-61.630 \pm 0.099	-69.039 \pm 0.057	-14.70 \pm 0.17	46.078 \pm 0.108	-1.858 \pm 0.006	
342	106353	6830027182179257472	323.096671	-20.957957	-279.074 \pm 0.103	-124.241 \pm 0.086	32.57 \pm 0.16	28.740 \pm 0.061		
	106350	6830027143525634432	323.086142	-20.970035	-284.665 \pm 0.091	-123.311 \pm 0.075	33.62 \pm 0.28	28.738 \pm 0.053	-2.107 \pm 0.004	
344	107299	6458951765971500672	325.995032	-57.325475	-116.563 \pm 0.062	-52.575 \pm 0.054	36.95 \pm 0.20	44.462 \pm 0.089		
	107300	6458952345790198144	326.000646	-57.283282	-115.298 \pm 0.049	-52.865 \pm 0.045	37.16 \pm 0.16	44.373 \pm 0.066	-1.484 \pm 0.002	
352	110084	6613555642140332672	334.478622	-32.479717	163.485 \pm 0.077	-203.690 \pm 0.078	-77.34 \pm 0.20	47.692 \pm 0.111		
	111520	6620882890706789248	338.918255	-28.133824	198.181 \pm 1.765	-163.762 \pm 1.749	1.78 \pm 0.54	51.467 \pm 2.529	0.700 \pm 0.023	d
359	112724	2211820991079869312	342.419369	66.199867	-63.663 \pm 0.625	-125.772 \pm 0.633		37.163 \pm 0.525		
	112324	2007431640735691776	343.264616	58.146467	-62.565 \pm 0.062	-135.767 \pm 0.059	-10.25 \pm 0.18	35.353 \pm 0.046	0.708 \pm 0.007	
366	114131	6541802406664428672	346.719425	-43.520412	-49.037 \pm 0.621	-13.454 \pm 0.651		36.046 \pm 0.634		
	114112	6541802578463122688	346.662879	-43.503830	-47.921 \pm 0.088	-22.151 \pm 0.100	15.37 \pm 0.23	40.237 \pm 0.143	-1.531 \pm 0.010	

Continued on next page

Index	HIP2	GDR2	α	δ	μ_α	μ_δ	v_r	d	$\log_{10}(\Delta R)$	Exclusion
SO11			(deg)		(mas/yr)		(km/s)	(pc)		Test
381	1266	2428524528072046464	3.966260	-8.876220	42.692±0.099	10.121±0.050	7.21± 0.26	98.401±0.465		
	118	2428948114926672128	0.386803	-9.430027	46.899±0.117	1.430±0.085	1.66± 0.26	78.579±0.471	0.742±0.005	c,d
384	2292	2526899001640197248	7.316650	-5.911442	-110.351±0.145	-221.185±0.071	9.54± 0.18	54.877±0.174		
	2350	2526925389919277056	7.499004	-5.764960	-107.019±0.094	-223.039±0.062	9.77± 0.27	55.049±0.155	-0.650±0.003	
392	4702	2356290256259997696	15.117303	-19.389626	128.469±0.101	-54.504±0.062	5.31± 0.16	82.225±0.309		
	4833	2356080043380354816	15.529355	-19.669909	129.340±0.085	-54.529±0.061	5.62± 0.19	81.436±0.274	-0.165±0.003	
402	6668	315635261093206656	21.393618	31.550204	156.296±0.086	-48.602±0.076	18.27± 0.20	63.089±0.207		
	6675	315635192373731328	21.411410	31.545948	155.319±0.086	-50.508±0.075		63.343±0.183	-1.760±0.004	
404	6772	4916890556306664192	21.776124	-51.965451	294.867±0.051	75.327±0.049	49.99± 0.18	56.705±0.096		
	6804	4916887395210737024	21.895937	-52.044359	294.046±0.032	75.068±0.033	50.23± 0.29	56.764±0.068	-0.971±0.001	
405	7189	4929377881661762944	23.151342	-49.728032	-28.252±0.047	-73.686±0.044	3.37± 0.37	81.153±0.209		
	7086	4929369360446613248	22.818624	-49.904326	-28.369±0.040	-75.405±0.044		81.000±0.207	-0.406±0.002	b
417	11137	76300510625993344	35.831622	15.419357	112.396±0.074	184.300±0.061	27.02± 0.15	60.120±0.132		
	11134	76300476266255488	35.821737	15.417794	111.098±0.064	183.174±0.050	27.30± 0.24	60.105±0.118	-1.994±0.004	
422	11736	2500621360930896640	37.871913	1.091259	-29.750±0.103	-23.012±0.082		107.030±0.560		
	12728	2498487861696380672	40.903989	-0.344632	-26.869±0.069	-25.355±0.073	9.73± 0.31	90.724±0.345	0.763±0.004	c
426	13223	31986240656172800	42.554350	13.710430	59.150±0.093	-8.651±0.090	-14.72± 15.28	94.865±0.546		
	13122	33216147491735808	42.195278	14.613596	58.013±0.088	-6.609±0.085	30.25± 0.21	76.807±0.280	0.161±0.004	c,d
427	13271	4949158198924394496	42.699429	-39.932267	41.760±0.052	-9.937±0.057		96.694±0.329		
	13499	4949081572411575552	43.466162	-40.194081	42.102±0.043	-6.409±0.047	18.12± 0.91	96.453±0.291	0.035±0.003	
441	15432	5047006006423053440	49.720802	-36.127117	37.017±0.040	-5.105±0.059		105.680±0.336		
	15152	5046487311812732544	48.821500	-37.041717	38.972±0.039	-5.318±0.057	17.59± 0.97	100.649±0.266	0.322±0.003	
445	16410	117916235464382336	52.833080	27.571643	38.561±0.106	-31.966±0.079		104.541±0.602		
	16742	69733883588579840	53.838995	26.852557	28.033±0.088	-31.248±0.069		195.915±1.768	0.478±0.007	c
448	16959	4728825002249947904	54.542882	-59.776194	26.094±0.042	43.356±0.047		76.949±0.139		
	16942	4728825036609672576	54.511235	-59.775713	25.698±0.199	44.655±0.207	9.03± 2.40	77.615±0.735	-1.668±0.008	
450	17486	4666907551119833984	56.195067	-70.027068	-10.234±0.043	-97.151±0.049	27.65± 0.14	55.118±0.069		
	17515	4666907516760096512	56.256345	-70.024519	-9.249±0.048	-97.358±0.050	27.94± 0.19	54.988±0.074	-1.693±0.002	
462	20109	4780193841901310336	64.667115	-52.859782	47.538±0.086	72.662±0.154		75.921±0.271		a
	20074	4780194185498710144	64.564161	-52.901991	49.705±0.061	73.646±0.100	21.51± 0.25	74.962±0.192	-1.005±0.003	
465	21537	3230677565443833088	69.361411	0.553169	16.653±0.102	11.603±0.057	38.60± 0.17	64.132±0.214		
	21534	3230677870385455232	69.358778	0.574687	15.953±0.100	12.163±0.054	38.97± 0.17	64.119±0.204	-1.615±0.003	
467	21704	2976981131534077056	69.904334	-21.247450	12.719±0.049	22.037±0.077	9.57± 0.16	83.375±0.300		
	21702	2976981337692506240	69.895710	-21.239607	12.411±0.042	22.892±0.046	7.96± 0.23	83.051±0.224	-1.788±0.005	
478	25453	3238066592819780608	81.661830	6.868519	9.167±0.097	-32.465±0.080		101.834±0.560		
	25483	3334161160308637312	81.750020	7.170142	9.341±0.102	-33.164±0.089		98.459±0.715	-0.260±0.006	
481	25711	3447142233536837376	82.352673	31.426028	-0.561±0.099	-46.080±0.069		75.565±0.284		
	25614	3447107495841475712	82.083455	31.048402	-2.399±0.088	-53.567±0.066	-21.34± 0.30	132.969±1.180	-0.094±0.006	c
484	26309	2907397747897070336	84.043022	-28.708027	25.325±0.054	-3.082±0.073		58.897±0.154		
	26453	2907308172059100544	84.415231	-28.626307	24.080±0.034	-3.100±0.041	26.05± 0.45	59.114±0.083	-0.460±0.002	
487	26680	3339560999352744960	85.048812	10.252564	-7.541±0.119	-28.727±0.092	29.53± 0.54	82.925±0.369		
	26646	3339565461821955712	84.946518	10.339045	-8.312±0.085	-29.008±0.069	30.69± 0.68	82.508±0.328	-0.718±0.004	
489	27069	3023084272561678976	86.106147	-5.464855	14.670±0.080	-23.036±0.085		87.312±0.462		
	26588	3017087261266087552	84.773120	-5.897631	15.729±0.086	-21.779±0.080	25.40± 0.74	89.594±0.410	0.333±0.004	
492	27791	3454470100579668992	88.219656	34.444815	-8.834±0.110	-71.574±0.089	-37.59± 5.29	89.428±0.675		a,b
	28872	3453690993510788480	91.436317	36.934039	-8.260±0.080	-70.593±0.066	25.30± 0.50	109.959±0.579	0.798±0.005	c,d
499	31323	3382205557837836288	98.529539	22.123988	-8.301±0.087	-35.555±0.073		94.444±0.524		a
	31316	3382205592197580928	98.515108	22.117513	-7.316±0.092	-34.348±0.076	-26.28± 0.30	94.856±0.524	-1.610±0.008	
510	35341	948509515477490560	109.509153	40.883448	-12.784±0.165	12.065±0.155		95.725±1.022		
	35799	974093501788080384	110.764196	45.000203	-11.563±0.064	-5.904±0.039	32.57± 0.27	1029.404±39.123	1.617±0.031	c
525	41081	5322206718812246656	125.729666	-52.123645	-23.039±0.140	-19.548±0.117		73.249±0.382		

Continued on next page

Index	HIP2	GDR2	α	δ	μ_α	μ_δ	v_r	d	$\log_{10}(\Delta R)$	Exclusion
SO11			(deg)		(mas/yr)		(km/s)	(pc)		Test
	40916	5320716335102626048	125.251760	-52.227884	-22.095 \pm 0.056	19.644 \pm 0.059		72.713 \pm 0.138	-0.402 \pm 0.003	
527	41880	3076534861386561536	128.092411	-0.937638	-133.683 \pm 0.073	83.519 \pm 0.053	15.31 \pm 0.29	69.099 \pm 0.201		
	41881	3076535243639085440	128.096341	-0.927400	-135.608 \pm 0.076	81.968 \pm 0.056	14.85 \pm 0.35	69.356 \pm 0.222	-1.878 \pm 0.003	
540	45811	5742852762061629056	140.120838	-9.555820	-12.896 \pm 0.462	-27.707 \pm 0.536	25.14 \pm 0.16	68.539 \pm 1.707		
	45802	5742848123496954112	140.087475	-9.610300	-13.982 \pm 0.178	-29.110 \pm 0.155	31.99 \pm 1.32	66.917 \pm 0.523	-1.124 \pm 0.015	d
541	45937	5310444491348428544	140.506149	-54.543106	18.112 \pm 0.055	120.947 \pm 0.055	91.12 \pm 0.16	67.899 \pm 0.139		
	45952	5310446621652246144	140.579963	-54.464723	22.511 \pm 0.108	114.544 \pm 0.121		67.493 \pm 0.238	-0.977 \pm 0.002	
542	46298	1131772432806417280	141.620478	78.437919	30.488 \pm 0.071	26.021 \pm 0.069	-10.71 \pm 0.18	53.853 \pm 0.117		
	46299	1131771646828736000	141.625549	78.429867	34.502 \pm 0.053	25.967 \pm 0.066	-11.18 \pm 0.21	53.877 \pm 0.096	-2.117 \pm 0.005	
546	47017	5249310751464090112	143.734891	-64.999265	-34.698 \pm 0.058	43.970 \pm 0.051	44.93 \pm 14.31	87.442 \pm 0.228		
	47351	5249282164160875136	144.725079	-64.990582	-34.905 \pm 0.051	41.369 \pm 0.050	22.62 \pm 1.01	90.548 \pm 0.222	-0.187 \pm 0.002	d
549	47231	1050821477623210368	144.406188	60.213545	-11.880 \pm 0.065	-32.046 \pm 0.053	9.19 \pm 0.13	112.655 \pm 0.488		
	46170	1038770314786277248	141.234404	59.993030	-17.608 \pm 0.054	-20.520 \pm 0.055	-19.63 \pm 0.28	103.250 \pm 0.378	0.478 \pm 0.003	d
550	47335	5247416705243609088	144.688027	-66.858881	-36.613 \pm 0.052	45.089 \pm 0.053		85.534 \pm 0.230		
	47017	5249310751464090112	143.734891	-64.999265	-34.698 \pm 0.058	43.970 \pm 0.051	44.93 \pm 14.31	87.442 \pm 0.228	0.458 \pm 0.002	
551	47399	813906786608830464	144.864275	42.285845	-6.119 \pm 0.063	-6.587 \pm 0.065	-3.36 \pm 0.48	74.017 \pm 0.272		
	47851	801608096216800000	146.304399	41.155079	-1.902 \pm 0.089	-3.864 \pm 0.100		370.751 \pm 9.574	0.782 \pm 0.019	c
557	51536	828983049535772928	157.894852	43.264808	-20.822 \pm 0.059	15.860 \pm 0.084		99.483 \pm 0.437		
	51726	828895294768816000	158.531822	43.464793	-11.095 \pm 0.080	8.714 \pm 0.105	-11.98 \pm 0.33	142.610 \pm 1.172	0.028 \pm 0.006	c
558	51608	5229614856076359168	158.134154	-72.428414	-56.798 \pm 0.047	-45.861 \pm 0.046	0.37 \pm 0.20	70.927 \pm 0.136		
	51611	5229612622693362048	158.145528	-72.441652	-56.698 \pm 0.043	-46.489 \pm 0.037	0.40 \pm 0.54	70.918 \pm 0.112	-1.771 \pm 0.002	
582	57950	5343610331876174336	178.283059	-56.727293	-39.410 \pm 0.058	-10.227 \pm 0.052	13.36 \pm 0.66	102.128 \pm 0.460		
	59716	6075548419252906368	183.711072	-55.789916	-35.722 \pm 0.050	-11.041 \pm 0.042	14.22 \pm 1.23	114.852 \pm 0.518	0.776 \pm 0.004	
588	58751	3575541998835891456	180.749457	-10.752474	33.041 \pm 0.105	-18.763 \pm 0.077	-12.39 \pm 0.20	57.262 \pm 0.183		
	58722	3575542995268304512	180.664538	-10.713711	33.067 \pm 0.840	-20.664 \pm 0.747	-16.16 \pm 0.70	54.426 \pm 1.115	-1.047 \pm 0.010	d
589	58813	6147474037517738624	180.943487	-44.122728	98.970 \pm 0.059	18.173 \pm 0.039	6.41 \pm 0.12	53.089 \pm 0.131		
	58815	6147474071877478144	180.949433	-44.117898	101.361 \pm 0.055	15.724 \pm 0.036	6.14 \pm 0.17	52.952 \pm 0.126	-2.224 \pm 0.010	b
592	59243	5788355123068307328	182.281096	-78.781346	-43.364 \pm 0.062	-7.619 \pm 0.060		99.808 \pm 0.327		
	58490	5224879500011370496	179.925399	-76.023964	-41.025 \pm 0.043	-6.190 \pm 0.038	12.63 \pm 1.40	99.746 \pm 0.231	0.689 \pm 0.002	
595	59865	6054216931644194304	184.157892	-63.197879	-145.407 \pm 0.046	6.329 \pm 0.041	-9.93 \pm 0.16	68.919 \pm 0.157		
	59913	6054219165008718848	184.342422	-63.226932	-145.829 \pm 0.047	7.784 \pm 0.045	-9.15 \pm 0.19	69.046 \pm 0.166	-0.974 \pm 0.002	
596	59898	5860789299912353024	184.275888	-65.693002	-38.331 \pm 0.083	-10.073 \pm 0.077		105.943 \pm 0.604		
	60183	5860587917472173056	185.117150	-65.842707	-41.434 \pm 0.100	-11.322 \pm 0.084		97.363 \pm 0.587	-0.175 \pm 0.005	
597	59960	6072902994276659200	184.471331	-55.975581	-39.014 \pm 0.057	-12.872 \pm 0.046		103.334 \pm 0.458		
	59716	6075548419252906368	183.711072	-55.789916	-35.722 \pm 0.050	-11.041 \pm 0.042	14.22 \pm 1.23	114.852 \pm 0.518	-0.053 \pm 0.004	
607	61135	3907637494456207360	187.913755	12.127870	-57.344 \pm 0.128	3.719 \pm 0.078		106.825 \pm 0.700		
	61416	3931759748777206272	188.777443	12.938992	-57.292 \pm 0.155	6.364 \pm 0.073	17.46 \pm 0.19	107.151 \pm 0.850	0.339 \pm 0.006	
610	61937	3927438771159865856	190.392833	10.426268	-106.518 \pm 0.092	-0.193 \pm 0.057		71.160 \pm 0.247		b
	62350	3927604694336986368	191.641939	11.378495	-112.544 \pm 0.114	-0.472 \pm 0.059	-17.49 \pm 0.14	65.405 \pm 0.297	0.267 \pm 0.003	
620	65466	1446271417351852544	201.277774	23.854387	-10.836 \pm 0.220	-7.596 \pm 0.194		90.650 \pm 0.841		
	65508	1448260262087566848	201.413988	25.682150	-10.309 \pm 0.088	-8.666 \pm 0.071	-0.35 \pm 0.66	86.755 \pm 0.292	0.453 \pm 0.006	
624	65779	5863709946382545280	202.275373	-66.073676	-127.902 \pm 0.048	11.368 \pm 0.056	-24.72 \pm 0.29	78.909 \pm 0.228		
	65785	5863709946382541952	202.289332	-66.078529	-127.318 \pm 0.041	11.056 \pm 0.050	-24.52 \pm 0.35	78.838 \pm 0.207	-1.989 \pm 0.008	
626	65899	1442870284289795968	202.628390	22.512881	25.400 \pm 0.076	-45.436 \pm 0.034	-35.48 \pm 0.18	83.756 \pm 0.263		
	65884	1441682158897145600	202.579217	21.500051	22.957 \pm 0.075	-49.366 \pm 0.032	58.12 \pm 0.30	87.091 \pm 0.277	0.179 \pm 0.003	d
630	66749	6293670601102816128	205.211181	-17.792721	-36.521 \pm 0.086	-11.333 \pm 0.079	-8.19 \pm 0.46	90.540 \pm 0.458		
	66717	6293764540627556224	205.135238	-17.343786	-45.844 \pm 0.116	-13.594 \pm 0.112	-1.02 \pm 0.51	108.416 \pm 1.021	-0.103 \pm 0.006	c,d
633	67250	149645690754708736	206.748323	38.542600	-134.290 \pm 0.088	-22.464 \pm 0.115	-11.20 \pm 0.13	92.492 \pm 0.788		
	67041	1496708798857641600	206.083788	38.797635	-141.262 \pm 0.026	-23.293 \pm 0.038	-32.94 \pm 0.18	95.946 \pm 0.296	-0.022 \pm 0.005	d
635	67470	3728726646011331328	207.399613	13.010410	-147.396 \pm 0.067	25.352 \pm 0.059		56.281 \pm 0.141		b
	67673	3728039760481678592	207.961829	11.937313	-149.496 \pm 0.077	25.658 \pm 0.055	-2.80 \pm 0.48	58.219 \pm 0.162	0.081 \pm 0.002	

Continued on next page

Index	HIP2	GDR2	α	δ	μ_α	μ_δ	v_r	d	$\log_{10}(\Delta R)$	Exclusion
SO11			(deg)		(mas/yr)		(km/s)	(pc)		Test
636	67639	6094716308525121408	207.884045	-48.293349	-114.076 \pm 0.108	-27.236 \pm 0.101	5.75 \pm 0.18	68.484 \pm 0.284		
	67645	6094716239805635072	207.893709	-48.298861	-113.740 \pm 0.104	-26.793 \pm 0.102	4.72 \pm 0.22	68.085 \pm 0.278	-1.996 \pm 0.013	
642	68830	6291206045789315328	211.410852	-18.072550	39.425 \pm 0.094	-45.424 \pm 0.076	15.18 \pm 12.84	88.382 \pm 0.436		
	68833	6291205977069837696	211.412416	-18.081112	37.270 \pm 0.094	-44.559 \pm 0.081	28.05 \pm 0.18	89.125 \pm 0.420	-1.871 \pm 0.008	d
655	71726	1282815063829295360	220.077109	30.443646	93.410 \pm 0.064	-44.363 \pm 0.086	-11.80 \pm 0.15	54.983 \pm 0.136		
	71737	1282817022334383232	220.118799	30.520323	93.470 \pm 0.073	-43.678 \pm 0.095	-11.49 \pm 0.14	54.724 \pm 0.156	-1.091 \pm 0.002	
677	76046	4414349489701257984	232.953494	-2.066574	-79.827 \pm 0.083	-30.371 \pm 0.071	-9.52 \pm 0.26	76.037 \pm 0.302		
	75923	4416093315142832128	232.604610	-1.318934	-70.150 \pm 0.072	-28.983 \pm 0.060	-25.82 \pm 1.27	67.463 \pm 0.203	0.014 \pm 0.003	d
678	76133	4416110082695309184	233.241330	-1.186582	-17.765 \pm 0.214	-42.217 \pm 0.205	-15.85 \pm 0.15	82.944 \pm 0.887		
	77728	4403070149671286656	238.052074	-2.278682	-15.408 \pm 0.093	-43.981 \pm 0.066	-3.50 \pm 0.26	88.630 \pm 0.468	0.868 \pm 0.007	d
691	78283	1202709349617637632	239.757321	18.325889	-59.445 \pm 0.065	2.520 \pm 0.058	-61.82 \pm 0.16	71.079 \pm 0.306		
	78067	1204270110670555136	239.094563	20.418776	-56.658 \pm 0.058	9.315 \pm 0.061	-18.21 \pm 0.71	80.184 \pm 0.321	0.460 \pm 0.004	d
704	80886	1299204074916904320	247.745828	23.985828	-30.683 \pm 0.041	31.931 \pm 0.050	-20.02 \pm 0.23	74.958 \pm 0.181		
	81875	1299508639637961344	250.861555	23.196612	-30.122 \pm 0.032	30.284 \pm 0.045	-40.40 \pm 0.29	99.969 \pm 0.249	0.655 \pm 0.002	c,d
707	81641	4434301983614947072	250.161198	4.219745	0.353 \pm 0.175	-10.476 \pm 0.134		101.209 \pm 1.084		
	81634	4434301841878055296	250.146462	4.207160	0.364 \pm 0.124	-9.859 \pm 0.095		99.832 \pm 0.640	-1.469 \pm 0.008	
713	84054	4571879578631697024	257.763126	24.237827	-11.782 \pm 0.054	30.655 \pm 0.056		80.848 \pm 0.272		
	84070	4571879475552172544	257.820456	24.252545	-11.230 \pm 0.037	29.770 \pm 0.042		79.667 \pm 0.190	-1.119 \pm 0.003	
715	84515	4388409330344765056	259.153687	3.408540	-60.249 \pm 0.072	19.568 \pm 0.063	-14.44 \pm 0.22	82.661 \pm 0.311		
	85911	4485937214320449280	263.339536	5.700825	-54.948 \pm 0.083	21.769 \pm 0.071	-22.79 \pm 0.29	73.460 \pm 0.234	0.812 \pm 0.003	d
726	85940	4487578544660527488	263.469996	8.103517	-16.092 \pm 0.099	-59.011 \pm 0.087	-28.07 \pm 0.18	90.978 \pm 0.397		b
	85944	4487581018562340992	263.483482	8.165793	-13.134 \pm 0.087	-60.275 \pm 0.084		90.133 \pm 0.337	-0.997 \pm 0.004	
737	88782	6719536193567989120	271.858999	-46.899274	-32.617 \pm 0.086	-106.932 \pm 0.081	-83.59 \pm 0.12	71.053 \pm 0.322		
	87887	5954345541675673728	269.293720	-46.122032	-43.037 \pm 0.096	-102.548 \pm 0.085	19.85 \pm 0.25	84.984 \pm 0.363	0.419 \pm 0.004	c,d
740	89373	6721441784663730816	273.581281	-43.154515	-0.873 \pm 0.104	-53.633 \pm 0.091	-44.16 \pm 0.33	103.306 \pm 0.605		
	89274	6724728980838829952	273.257554	-42.288522	-5.729 \pm 0.101	-51.286 \pm 0.087		109.826 \pm 0.798	0.223 \pm 0.006	
743	90026	6649398690418063232	275.541876	-55.564195	77.717 \pm 0.075	1.586 \pm 0.076		96.083 \pm 0.534		
	90028	6649398690418059392	275.542705	-55.572839	79.534 \pm 0.073	1.748 \pm 0.068	-5.14 \pm 0.16	96.934 \pm 0.538	-1.836 \pm 0.013	
749	93029	2133995118527034496	284.270902	51.720942	43.638 \pm 0.057	-5.617 \pm 0.055	1.76 \pm 0.46	84.236 \pm 0.185		
	92467	2143913950359678464	282.666306	49.767527	45.000 \pm 0.042	-1.773 \pm 0.051	-12.52 \pm 0.40	86.532 \pm 0.173	0.516 \pm 0.002	d
756	96979	4301163357576782464	295.691253	8.382994	23.989 \pm 0.081	53.912 \pm 0.053	-40.83 \pm 0.17	60.953 \pm 0.220		
	96976	4301163323217046912	295.684014	8.380594	23.964 \pm 0.074	52.346 \pm 0.050	-41.00 \pm 0.16	60.950 \pm 0.186	-2.095 \pm 0.005	
759	97646	6447036152303430528	297.686877	-59.193721	23.300 \pm 0.463	-12.433 \pm 0.407		85.947 \pm 2.503		
	97581	6447030139349235200	297.514014	-59.264087	24.031 \pm 0.114	-15.899 \pm 0.082		91.402 \pm 0.617	-0.757 \pm 0.015	
761	98174	6447100091479968256	299.276478	-58.901415	23.248 \pm 0.230	-14.783 \pm 0.246		90.149 \pm 1.382		
	97646	6447036152303430528	297.686877	-59.193721	23.300 \pm 0.463	-12.433 \pm 0.407		85.947 \pm 2.503	0.125 \pm 0.019	
768	99689	1808691203160200576	303.437164	16.157968	-7.280 \pm 1.319	5.631 \pm 1.216		124.509 \pm 12.288		
	100451	1808808571723073152	305.555561	16.372994	1.538 \pm 0.067	0.497 \pm 0.060		328.737 \pm 4.829	0.908 \pm 0.033	c
770	99729	4249652990144051840	303.540141	6.588725	-132.528 \pm 0.101	-58.445 \pm 0.064	-0.18 \pm 0.20	63.078 \pm 0.208		
	99727	4249652783985617920	303.537683	6.576958	-129.729 \pm 0.096	-59.388 \pm 0.065	-0.21 \pm 0.19	63.093 \pm 0.203	-1.878 \pm 0.004	
776	100941	6679307846231740032	306.999982	-42.620131	94.662 \pm 0.082	-122.858 \pm 0.057		104.908 \pm 0.685		
	100937	6679308018030433536	306.986590	-42.620666	93.796 \pm 0.078	-122.511 \pm 0.055	-62.19 \pm 0.23	105.016 \pm 0.629	-1.743 \pm 0.009	
777	101082	2298101352139398144	307.366686	81.092228	66.243 \pm 0.082	221.381 \pm 0.105	-14.38 \pm 0.17	64.364 \pm 0.211		
	101166	2298101901895214720	307.593111	81.140436	66.494 \pm 0.058	221.043 \pm 0.070	-14.24 \pm 0.27	64.049 \pm 0.124	-1.176 \pm 0.002	
780	101719	2195226749280378368	309.283271	61.364403	23.834 \pm 0.051	-42.621 \pm 0.048	3.21 \pm 0.18	57.493 \pm 0.082		
	102727	2194321816851242624	312.239000	61.118583	19.428 \pm 0.053	-40.421 \pm 0.050	-9.36 \pm 0.18	65.332 \pm 0.122	0.189 \pm 0.001	d
782	102725	6376446646806738816	312.236006	-68.791520	42.026 \pm 0.043	-61.530 \pm 0.069		85.988 \pm 0.270		
	103917	6375793502540188800	315.826134	-69.171496	44.104 \pm 0.053	-59.448 \pm 0.055	-10.04 \pm 0.17	87.808 \pm 0.446	0.309 \pm 0.004	
784	103107	6481251098731588224	313.358335	-49.383030	43.599 \pm 0.064	-30.438 \pm 0.051	-16.94 \pm 0.28	89.053 \pm 0.300		
	103139	6481246906845850880	313.465930	-49.449714	43.875 \pm 0.051	-27.428 \pm 0.044	-17.98 \pm 0.43	89.993 \pm 0.292	-0.821 \pm 0.003	
793	104536	1839746393680655232	317.629011	22.457052	22.239 \pm 0.137	-11.888 \pm 0.138		116.759 \pm 1.188		

Continued on next page

Index	HIP2	GDR2	α	δ	μ_α	μ_δ	v_r	d	$\log_{10}(\Delta R)$	Exclusion
SO11			(deg)		(mas/yr)		(km/s)	(pc)		Test
	102981	1838905954482116480	312.957870	21.868618	20.705 \pm 0.081	-11.991 \pm 0.072	-11.55 \pm 0.18	108.378 \pm 0.582	0.933 \pm 0.007	
802	109306	6611824083124944384	332.177751	-33.125589	13.261 \pm 0.078	24.447 \pm 0.081		78.654 \pm 0.344		
	110433	6599619950733282304	335.519158	-34.488798	11.670 \pm 0.060	25.950 \pm 0.066		86.438 \pm 0.281	0.649 \pm 0.003	
815	112537	2396293134977302272	341.906431	-23.172364	24.576 \pm 0.071	-10.583 \pm 0.065	-3.25 \pm 0.37	78.726 \pm 0.286		
	111596	6628071944405827712	339.129743	-21.584986	31.319 \pm 0.072	-4.837 \pm 0.062	11.06 \pm 1.60	106.288 \pm 0.444	0.688 \pm 0.003	c,d
839	117454	2337899270721594752	357.237150	-25.144889	-13.177 \pm 0.093	-42.966 \pm 0.111	-3.30 \pm 0.83	85.714 \pm 0.686		
	117720	2338428513772452480	358.123916	-24.165778	-15.355 \pm 0.095	-39.481 \pm 0.069	44.28 \pm 0.67	113.458 \pm 0.771	0.343 \pm 0.006	c,d

Table 1: *Hipparcos* and Gaia identification numbers for the 133 binary stars used, together with Gaia DR2 data and results of the exclusion tests performed: (a) shows an individual star excluded (which results in the exclusion of the respective binary) for having an inconsistent proper motion in right ascension between *Hipparcos* and the DR2, (b) the corresponding result for declination, (c) shows a binary excluded for having discordant parallaxes to both components (distance differences larger than 13 %) in the DR2 data, and (d) gives binaries removed for having DR2 radial velocity differences $> 4 \text{ km s}^{-1}$, with the 81 retained binaries appearing blank in this column. Upper rows give data of primaries and lower ones of secondaries.

Acknowledgments

The authors thank an anonymous referee for a careful reading of the first version of this paper and constructive criticism leading to a more complete and clearer final version. XH and RAMC acknowledge the support of DGAPA-UNAM PAPIIT IN-104517 and CONACyT.

References

1. Koposov S. E. et al., *ApJ* **811** (2015) 62
2. Salucci P., Wilkinson M. I., Walker M. G., Gilmore G. F., Grebel E. K., Koch A., Frigerio M. C. & Wyse R. F. G., *MNRAS* **420** (2012) 2034
3. Lelli F., McGaugh S. S. & Schombert J. M., *MNRAS* **468** (2017) L68
4. Durazo R., Hernandez X., Cervantes Sodi B., & Sanchez, S. F., *ApJ* **863** (2018) 107
5. Scarpa R., Marconi G. & Gilmozzi R., *A&A* **405** (2003) L15
6. Scarpa R., Marconi G., Carraro G., Falomo R. & Villanova S., *A&A* **525** (2011) A148
7. Milgrom M., *ApJ* **287** (1984) 571
8. Sanders R. H. & McGaugh S. S., *ARA&A* **40** (2002) 263
9. Hernandez X., Jimenez M. A. & Allen C., *Eur. Phys. J. C* **72** (2012) 1884
10. Shaya E. J. & Olling R. P., *ApJS* **192** (2011) 2
11. Jiang Y.-F. & Tremaine S., *MNRAS* **401** (2010) 977
12. Scarpa R., Ottolina R., Falomo R., Treves A., *Int. J. Mod. Phys.* **26** (2017) 1750067
13. Pittordis C. & Sutherland W., *MNRAS* **480** (2018) 1778
14. Banik I. & Zhao H., *MNRAS* **480** (2018) 2660
15. Marrese P. M., Marinoni S., Fabrizio M. & Altavilla G., *arXiv:180809151* (2018)
16. Gaia Collaboration, *A&A* **616** (2018) 1
17. Høg E., et al., *A&A* **357** (2000) 367
18. Fabricius C., Høg E., Makarov V.V., Mason B.D., Wycoff G.L. & Urban S.E., *A&A* **384** (2002) 180
19. Smart W. M., 1968, *Stellar Kinematics*. Longmans, London
20. Oh S., Price-Whelan A. M., Hogg D. W., Morton T. D. & Spergel D. N., *AJ* **153** (2017) 257
21. Milgrom, M., *AcPPB* **42** (2011) 2175
22. Capozziello, S., & De Laurentis, M., *PhR* **509** (2011) 167
23. Verlinde, E., *SciPostPhys* **2** (2017) 016
24. Barrientos, E., & Mendoza, S., *Phys. Rev. D* **98** (2018) 084033